Proceedings of the 1986 Winter Simulation Conference
J. Wilson, J. Henriksen, S. Roberts (eds.)

MODELING THE INITIALIZATION PROCESS OF A SPACE-LAUNCHED KINETIC ENERGY WEAPON

William A. Laidig
Harold L. Pastrick
Science Applications International Corporation
2109 Clinton Avenue, West, Suite 800, Huntsville, AL 35805-3008

ABSTRACT

A six degree-of-freedom simulation modeling an SDI space-based kinetic energy weapon is examined to analyze the models which represent the interceptor component initialization scheme. The initialization scheme consists of the first downlink of target information from the radar platform to the launch platform, the handing down of launch platform initial parameters to the interceptor, the predicted impact point algorithm and launcher training, and the interceptor on-board Kalman filter and target predictor start-up procedure. These conceptual models are defined and associated error sources are applied. The impact of the initialization errors on the kinetic energy weapon system performance, as dictated by six degree-of-freedom simulation test runs, is discussed.

1. INTRODUCTION

The Strategic Defense Initiative (SDI) program is composed of several key technology areas, each with the task of analyzing the necessity and effectiveness of a layered system of defense against ballistic missile attack. The ICBM journey begins with a powered boost period lasting several minutes. After burnout, the missile deploys its bussed cargo of nuclear warheads, decoys and penetration aids; this phase is referred to as the post boost phase. The released cargo then travels a lofty ballistic trajectory back to the earth's atmosphere during the midcourse phase of flight. During the terminal phase, the reentry vehicles pass through the atmosphere, at which time the lighter decoys begin to fall behind and burn while the warheads continue toward their pre-appointed targets. The tiered levels of defense represent a variety of methods proposed to engage and destroy ICBMs and their payloads during all phases of flight. Using such tools as computer simulations, the Strategic Defense Initiative seeks to develop sound technical options that could lay the ground work for an effective defense against the ballistic missile.

One such technology area of interest is the kinetic energy weapon study. Kinetic energy weapons include interceptor missiles and hyper-velocity gun systems which will rely on non-nuclear kill mechanisms to destroy the intended target. The primary roles for these defensive weapons include (1) midcourse engagement of re-entry vehicles (RVs) not destroyed during boost or post-boost phases, and of post-boost vehicles that have not dispensed all of the RVs; (2) terminal (i.e., endoatmospheric or within the atmosphere) engagement of RVs not destroyed during the previous phases of flight; (3) space platform defense against threats not vulnerable to directed energy weapons, and (4) boost-phase engagements of short time-of-flight, short-range, submarine-launched ballistic missiles. Additional roles for these defensive weapons include (1) boost phase intercept from space-based platforms, and (2) midcourse engagement from space-based platforms. The kinetic energy weapon boost phase intercept scenario, shown by the boost phase ICBM's (#1 in Figure 1), the orbiting launch platform (#2 in Figure 1), and the radar platform in geosynchronous orbit (#3 in Figure 1), encompasses the basis of this paper.

Figure 1 : The SDI Boost Phase Intercept Scenario

This paper will strive to describe the initialization process used to simulate the kinetic energy weapon residing on an orbiting platform by highlighting the key concerns and corresponding models that arise during simulation of the initialization process. The areas covered in this analysis include the radar platform and launch platform downlinks, the interceptor INU (Inertial Navigation Unit) start-up, the target predictor and pointing algorithm, the interceptor on-board target predictor and Kalman filter, and the impact of these erroneous processes on the kinetic energy weapon performance.

2. SIX DEGREE-OF-FREEDOM SIMULATION

In order to begin developing trade studies in the area of kinetic energy weapons, simulations are currently under various phases of construction to emulate the SDI architecture. One such simulation has been completed to model the kinetic energy weapon architecture as pictured in Figure 1. The full six degree-of-freedom simulation recreates the interceptor's flight from target acquisition to intercept. A simplified block diagram of the simulation contents is shown in Figure 2.

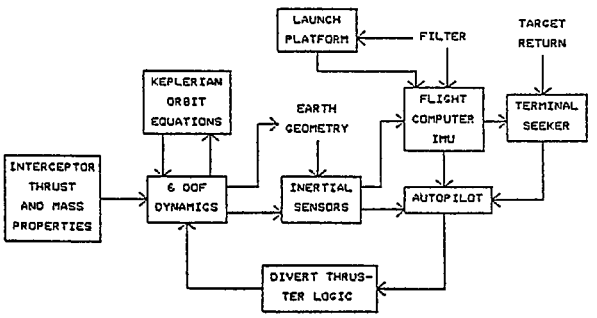

Figure 2: Six Degree-of-Freedom Logic Block Diagram

The difficulty in this study lies not in the development of suitable computer simulation models, but rather in bounding the problem to permit simulation excursions that will support specific hardware requirment recommendations. The following exemplifies the problem: Architectures have been derived that place the launch platform in nominal orbits of 500 km for the first two tiers, i.e., boost and post-boost phase engagements. But the same architecture suggests that midcourse engagements may be more effective with platforms at altitudes of over 1000 km. Couple that with threat scenarios that show several hundred seconds of target boost to those in the order of only 100 sec; fire controlled interceptor launches varying from 60 seconds after boost to just 10 seconds before end of boost phase; hot plume signatures on the booster to cooled deployed RVs with attended decoys and other penaids, yeild a parameter set that quickly can become unwieldly (Adam and Wallich, 1985). The initialization process used in the six degree-of-freedom simulation recreates a justifiable start-up procedure for the interceptor while at the same time adding suitable error sources to the interceptor's starting conditions in order to build a

strong baseline for necessary simulation excursions.

3. RADAR PLATFORM AND LAUNCH PLATFORM DOWNLINKS

For the purpose of discussing the computer modeling, it can be assumed that a radar platform in geosynchronous orbit exists in order to pass along target tracking information. Below the radar platform is assumed to be an orbiting platform capable of launching multiple interceptors toward various spotted targets. This concept, previously described, is pictured in Figure 1 above. When a target is acquired, the radar platform chooses the launch platform at the proper location in orbit and downlinks the target parameters to the chosen launch platform. The target parameters may include many components; however, in the six degree-of-freedom simulation models, the target position and velocity vectors relative to a common reference frame make up the entire initializing downlink message from the radar platform. After the initial downlink message, no target velocity is transmitted to the interceptor as its on-board filter and predictor system numerically differentiates the target position in order to obtain velocity. Random errors corrupt the target position and velocity measurements passed to the interceptor from the radar platform so as to simulate the radar uncertainties and communication related errors. The newly spotted target parameters from the radar platform downlink make up half of the interceptor initialization-necessary information. The second half includes the interceptor's present position, velocity, and acceleration vectors necessary for determining relative target information. It is assumed that the launch platform is aware of its position, velocity, and acceleration and need not get that information from an outside source. The launch platform therefore, is given the task of handing the interceptor information about its present position and heading from the launch platform's internal navigation components. The launch platform itself is travelling in a pre-designated orbit around the earth and therefore the on-board interceptor has a continuously changing position, velocity and acceleration before it is launched. The launch platform's position is tracked internally via its own INU consisting of rate gyros and accelerometers positioned such as to determine translational and rotational motion about all three axes. Because the launch platform is able to track its own position, the interceptor inertial navigation unit can be set to match that of the launch platform. Ideally, the transfer of information between the launch platform and the interceptor is assumed to be perfect. However, the navigation information aboard the launch platform contains errors. The initial Euler angles used in the interceptor's INU (for vehicle attitude information with respect to a relative axis system) are modeled as random errors representing the erroneous launch platform navigation parameters. The target and interceptor initial position parameters complete the simulation baseline start-up parameter definition.

4. INTERCEPTOR INU START-UP

In terms of the six degree-of-freedom simulation, the interceptor INU start-up procedure must first define the orbit of the launch platform. The launch platform's elliptical orbit can be described and predicted with Keplarian equations of motion as presented below. The launch platform's initial position and velocity vectors with respect to a fixed set of axes is the first step in the modeling process. An initial launch platform radius and velocity vector with respect to a set of axes fixed at the center of the earth (chosen to be the origin of the Inertial Coordinate System) was chosen and the parameters describing the orbit obtained from these vectors. Alternatively, the platform orbit parameters can be defined and the platform range and velocity vector can be determined from these preset orbit parameters. Either method is

acceptable depending upon the amount of information available. For the purpose of discussion, it was assumed that an initial radius and velocity vector comprise the information available, from which the orbital parameters were determined. The initial range and velocity were then extrapolated to represent the platform at some time past that initial time.

Given the platform initial range and velocity vectors ($\bar{r}$ and $\bar{v}$) the angular momentum obtained in the orbit was found from Bate, Mueller and White, 1971 by crossing the range and velocity vectors as shown.

$$\bar{h} = \bar{r} \times \bar{v} \tag{1}$$

Half the width of the eliptical orbit, at the prime focus, the semi-latus rectum (P), was found by dividing the magnitude of the momentum squared (from 1) by the Earth's gravitational parameter as shown.

$$P = \frac{|h|^2}{\mu} \tag{2}$$

The description of a conic trajectory is given by its eccentricity. The eccentricity vector is a vector with the magnitude of the conic eccentricity and directed toward the point nearest the prime focus or periapsis. The eccentricity vector describing the launch platform's trajectory was found as a function of mu, the initial platform radius and velocity vectors as shown below.

$$\bar{e} = \frac{1}{\mu}\left[\left(V^2 - \frac{\mu}{r}\right)\bar{r} - (\bar{r} \cdot \bar{V})\bar{V}\right] \tag{3}$$

The orbit's semi-major axis (a) was defined as a function of the semi-latus rectum and the eccentricity magnitude as shown.

$$a = \frac{P}{1 - |e|^2} \tag{4}$$

With equations 2, 3, and 4, the in-plane orbit parameters have all been defined. What remains to be shown is the inclination of that planar orbit with respect to a set of fixed axes and where on that planar orbit the launch platform resides during the initialization of the interceptor. As mentioned previously, the reference point for the launch platform's orbit (and prime focus) is the Inertial Coordinate System. The set of axes defined in the six degree-of-freedom simulation were positioned in such a way as to represent the freezing of the axes at some initial time (epoch) with the origin of the ICS (Inertial Coordinate System) embedded in the center of the earth and its I axis pointing toward the vernal equinox direction at epoch. The inertial J axis points 90 degrees to the east of the I axis within the equatorial plane, and the K axis completes the right hand rule and points up through the north pole. The Inertial Coordinate System as described is pictured below in Figure 3.

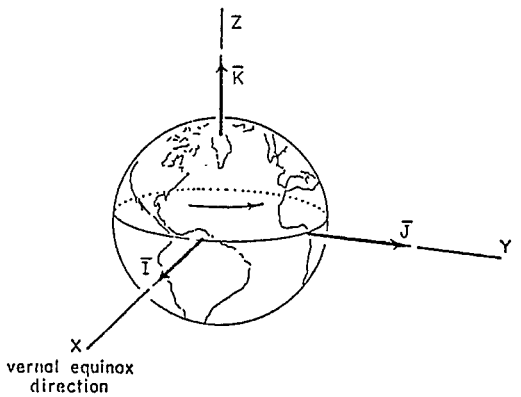

Figure 3: Chosen Inertial Coordinate System

The inclination angle (i) is defined as the angle between the momentum vector (which is perpendicular to the orbital plane) and the K unit vector of the inertial axis as can be seen below in Figure 4 from Bate, Mueller, and White, 1971.

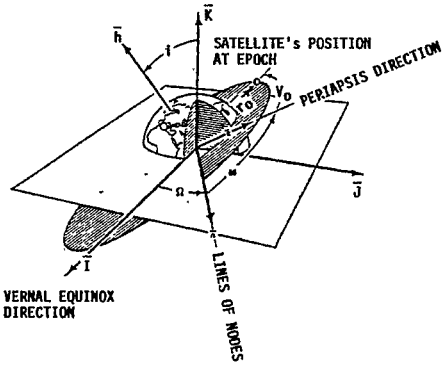

Figure 4: Definition of Orbital Plane With Respect to Inertial Coordinates

The inclination angle (i) was obtained using the expression:

$$i = \cos^{-1} \frac{h_K}{|h|}$$

The angular rotation of the platform in its orbit from the point of periapsis is known as its true anamoly (γ) as shown in Figure 4 and determined as:

$$\gamma = \cos^{-1} \left(\frac{\bar{e} \cdot \bar{r}}{er} \right).$$

These orbital parameters defined the trajectory of the platform at any time past epoch. In order to predict the position and velocity of the platform as it orbited the earth, the universal variable approach was employed to solve the Kepler problem. A time-of-flight equation was used to predict the change in platform position and velocity. The essence of the solution to the prediction problem is presented as follows: Given the launch platform's radius and velocity vectors in inertial coordinates, the semi-major axis (a), and the time difference between epoch and the future prediction time, the universal time-of-flight equation was resolved using Newton's iteration scheme to converge on the solution. The time-of-flight was determined with the solution of the following equation:

$$t_n = \frac{r_o \cdot V_o}{\mu} X_n^2 C + \frac{(1 - \frac{r_o}{a})}{\sqrt{\mu}} X_n^3 S + \frac{r_o X_n}{\sqrt{\mu}} \qquad (5)$$

When X_n was first determined with the approximation:

$$X_o = \frac{\Delta t}{a} \sqrt{\mu} . \qquad (6)$$

And C, S and Z were defined as

$$C = \sum_{K=0}^{\infty} \frac{(-Z)^K}{(2K+2)!} \qquad (7)$$

$$S = \sum_{K=0}^{\infty} \frac{(-Z)^K}{(2K+3)!} \qquad (8)$$

$$Z = \frac{X^2}{a} . \qquad (9)$$

The derivative of the time-of-flight with respect to the universal variable (X) can be shown to be:

$$\frac{dt}{dx} = \frac{X^2 C}{\sqrt{\mu}} + \frac{r_o \cdot V_o}{\mu} X_n (1 - ZS) + r_o (1 - ZC) . \qquad (10)$$

Newton's iteration scheme was used to make a better approximation for the universal variable as shown in equation 13.

$$x_{n+1} = X_n + \frac{\Delta t - t_n}{\left. \frac{dt}{dx} \right|_{X=X_n}} \qquad (11)$$

The above sequence (equations 5 - 11) was repeated until the iteration scheme converged, within a preset threshold, on the universal variable. Once this information was obtained, the new platform radius was found.

$$r = f r_o + g V_o$$

Where f and g were defined as follows:

$$f = 1 - \frac{X^2}{r_o} C$$

$$g = \Delta t - \frac{X^3}{\sqrt{\mu}} S .$$

The platform velocity at the prediction time was found using the following equation:

$$V = \dot{f} r_o + \dot{g} V_o .$$

Where $\dot{f}$ and $\dot{g}$ were as shown below in 12 and 13. Note that the platform initial radius vector (r_o) and the newly formed platform radius vector (r) were both used in the formulation of $\dot{f}$ and $\dot{g}$.

$$\dot{f} = \frac{\sqrt{\mu}}{r_o r} X(ZS-1) \qquad (12)$$

$$\dot{g} = 1 - \frac{X^2}{r} C \qquad (13)$$

With the ability to predict the platform's position and velocity at any time, the interceptor's on-board navigation unit was initialized and corresponding errors applied. The interceptor, having been passed information about its present position and velocity including error sources modeling the launch platform's inaccuracies, used a discrete update method to keep track of its position along and rotations about its body X, Y, and Z axes. Measurements obtained from the interceptor's on-board inertial measurement package were used to update this incremental navigation indicator. The information passed to the guidance computer from the measurement package was modeled to include several misalignment and operational errors.

The measurement package consisted of two sets of rate gyros and two sets of accelerometers mounted together in the package casing in such a way as to sense rotational rates (from the gyros) about the roll (X) axis, the pitch (Y) axis, and the yaw (Z) axis and accelerations along the X, Y, and Z body axes. Since two sets of each sensor are modeled, one redundant output is obtained and discarded. Regarding misalignment errors, the measurement package was mounted on the interceptor in such a way as to allow a very small error between the case relative axis and the interceptor body coordinate system. This unintentional misalignment may occur in all three axes of rotation. Internally, the sensor spin axis was misaligned with the sensor case relative axis for both sets of sensors as described in TASC Report, 1981. The spin axis misalignment can be seen from the Figure 5 below.

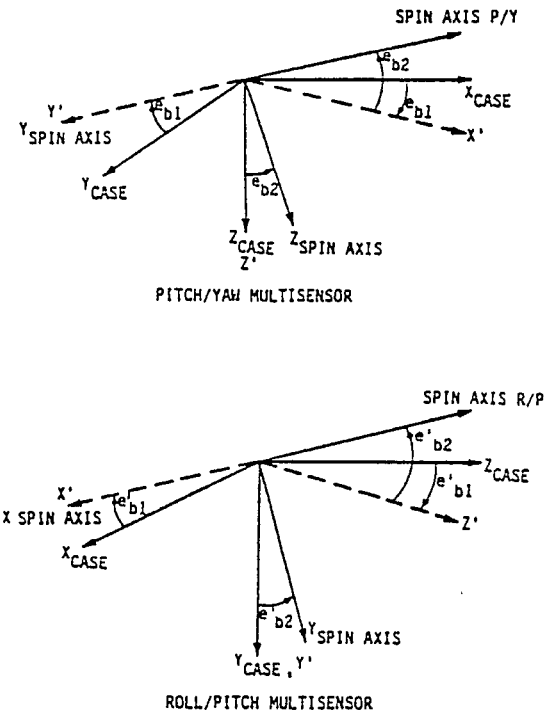

Figure 5: Multisensor Spin Axis Misalignment Defined

The misalignment e_{b1} is a rotation about Z_{case} to form the primed set of axes. The misalignment e_{b2} is a rotation about the Y' axis to form the SPIN AXIS, $Y_{spin\ axis}$, $Z_{spin\ axis}$ for the pitch/yaw sensor. The misalignment e_{b1}' is a rotation about Y_{case} to form X', Y', and Z' for the roll/pitch sensor. The misalignment e_{b2}' is a rotation about X' to form the $X_{spin\ axis}$, $Y_{spin\ axis}$, and SPIN AXIS for the roll/pitch sensor. The transformation including the sensor relative axis misalignment with the sensor case (denoted phi, theta, and psi) from interceptor body to the spin axis is given in equation 14 (employing small angle approximations).

$$\begin{bmatrix} \text{SPIN AXIS} \\ y_{\text{spin axis}} \\ z_{\text{spin axis}} \end{bmatrix} = \begin{bmatrix} 1 & e_{b1}+\psi & -e_{b2}-\theta \\ -e_{b1}-\psi & 1 & \phi \\ e_{b2}+\theta & -\phi & 1 \end{bmatrix} \begin{bmatrix} x \\ y \\ z \end{bmatrix}_{BCS} . \quad (14)$$

The acceleration sensor output axes were in a plane which is orthogonal to the spin axis. The output axes were assumed to be defined electronically and the axis resolution had an in-plane drift as a function of temperature. This error is denoted as e_{aA} in the acceleration sensing plane. Also, the output axes within the acceleration sensing plane were typically non-orthogonal. This non-orthogonality was specified by e_{oA} in the acceleration plane. The composite transformation from the interceptor body axis to the acceleration sensing axis can be shown to be as follows in 15.

$$\begin{bmatrix} \text{SPIN AXIS} \\ \eta_2 \\ \eta_3 \end{bmatrix} = \begin{bmatrix} 1 & e_{b1}+\psi & -e_{b2}-\theta \\ -e_{b1}-\psi & 1 & e_{aA}+\phi \\ e_{b2}+\theta & -e_{oA}-e_{aA}-\phi & 1 \end{bmatrix} \begin{bmatrix} \eta_x \\ \eta_y \\ \eta_z \end{bmatrix}_{BCS}$$

$$\eta_1 = \begin{bmatrix} 1 & e_{aA}'+\psi & -e_{b1}'-\theta \end{bmatrix} \begin{bmatrix} \eta_x \\ \eta_y \\ \eta_z \end{bmatrix}_{BCS} . \quad (15)$$

The interceptor body-to-rate sensing axis modeling followed the same logic as did the interceptor body-to-acceleration sensing axes transformation examined above. Thus the interceptor body-to-rate sensing axis modeling is not repeated here.

5. TARGET PREDICTION AND POINTING ALGORITHM

The second phase of the interceptor initialization procedure was the aiming of the interceptor toward some predicted impact point. The predicted impact point was determined using the following logic: The relative position and velocity of the target with respect to the platform were determined by subtracting the interceptor velocity and position, as seen in a common reference frame, from the target velocity and position. Refering to the vector diagram in Figure 6, the magnitude of the initial range vector from interceptor to target added to the range vector of the target's predicted trajectory (determined by multiplying the target velocity vector by the intercept time) was set equal to the pointing vector magnitude of the interceptor (defined as the interceptor's average velocity times the intercept time).

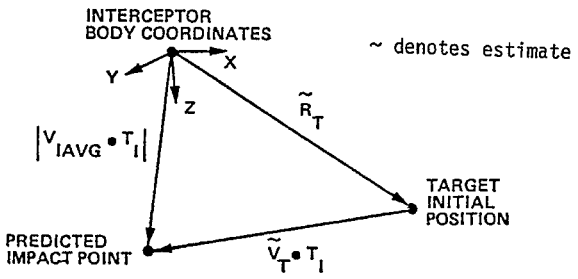

Figure 6: Predicted Impact Point Geometry

The algebraic interpretation of the above geometry follows as:

$$\left|\tilde{R}_T + \tilde{V}_T T_I\right| = \left|V_{IAVG} T_I\right| . \quad (16)$$

The solution of the vector equality (16) for the intercept time was given as:

$$T_1 = \tilde{V}_T \cdot \tilde{R}_T \quad (17)$$

$$T_2 = |\tilde{V}_T|^2 \quad (18)$$

$$T_I = \frac{T_1 + \sqrt{T_1^2 + |\tilde{R}_T|^2 (V_{I\,AVG}^2 - T_2)}}{V_{I\,AVG}^2 - T_2} . \quad (19)$$

The aimpoint (assuming no target maneuvering during the interceptor initialization period) was determined by propogating the target to its future position at intercept time as shown below using 17 - 19 above.

$$X_{TI} = \tilde{R}_{XT} + \tilde{V}_{XT} \cdot T_I$$

$$Y_{TI} = \tilde{R}_{YT} + \tilde{V}_{YT} \cdot T_I$$

$$Z_{TI} = \tilde{R}_{ZT} + \tilde{V}_{ZT} \cdot T_I$$

The launcher then slewed and elevated the interceptor to the proper position and ignited the vehicle's main boosters sending

the interceptor toward the predicted aimpoint.

The error associated with target uncertainty, as passed to the launch platform by the radar platform, created one type of error involved in the predicted impact point calculation. Another error in determining the impact point was the interceptor/launch platform's initial position and velocity vectors caused both by the erroneous handover from launch platform to interceptor and the on-board errors in the inertial measurement unit. Both uncertainties were fed directly into the pointing algorithm and therefore had a sizeable impact on the KEW system performance. Once the predicted impact point had been determined, the physical slewing and elevating of the launcher subsystem was to be modeled. The apparatus for accomplishing this movement also contained misalignment and pointing errors and proper error values were applied to the output angles obtained via the pointing algorithm to accomodate the physical launcher capabilities.

6. ON-BOARD PREDICTOR AND KALMAN FILTER

The third phase of the initialization procedure involved the initialization of the on-board predictor/filter algorithm which employed a Kalman filter. The predictor was necessary to extrapolate discrete radar platform downlinks which contains target parameters. The radar platform downlinks were available within some pre-designated discrete time interval; however, the inertially guided interceptor was able to predict the moving target's parameters between radar scans. The on-board Kalman filter was used to extrapolate the radar downlink, which contained only target position after initialization, to obtain target velocity and acceleration. The Kalman filter was also used to separate the radar downlink message from added noise elements.

The initialization of the target predictor was very simple as the 9 target states (X, Y, and Z axis position, velocity, and acceleration) were all set to zero. The Kalman filter was used to force the initialized predictor to converge upon the first radar measurement and was subsequently updated.

The initialization of the Kalman filter was assumed to be more complex. Three methods were submitted as possible initialization routines for the 9 filter states and their corresponding initial error covariance matrix. The first method relied on the radar platform for only one downlink to determine target position only. The resulting state vector is given below from Gelb, 1974.

$$\underline{\hat{x}}(0) = \begin{bmatrix} x_t \\ y_t \\ z_t \\ \dot{x}_t \\ \dot{y}_t \\ \dot{z}_t \\ \ddot{x}_t \\ \ddot{y}_t \\ \ddot{z}_t \end{bmatrix} = \begin{bmatrix} x_{tr} \\ y_{tr} \\ z_{tr} \\ AV_t\cos(\psi_A)\cos(\theta_A) \\ AV_t\sin(\psi_A)\cos(\theta_A) \\ AV_t\sin(\theta_A) \\ 0. \\ 0. \\ 0. \end{bmatrix}$$

Where (X_{tr}, Y_{tr}, Z_{tr}) was the target position vector measured by the radar and AV_t, psi_A, and $theta_A$ were the assumed target velocity, heading and elevation angles. The initial error covariance matrix was formed as follows:

$$P_{0x} = \begin{bmatrix} R_x & 0 & 0 \\ 0 & \sigma^2_x & 0 \\ 0 & 0 & \beta^2_x \end{bmatrix}, P_{0y} = \begin{bmatrix} R_y & 0 & 0 \\ 0 & \sigma^2_y & 0 \\ 0 & 0 & \beta^2_y \end{bmatrix}, P_{0z} = \begin{bmatrix} R_z & 0 & 0 \\ 0 & \sigma^2_z & 0 \\ 0 & 0 & \beta^2_z \end{bmatrix}.$$

When R_X was the position error variance, $sigma_X$ was the velocity error variance, and $beta_X$ was the acceleration error variance. The second initialization scheme required two radar measurements. The initial target velocity was estimated from the first two target position measurements and the initial target position was taken from the second radar downlink. The target velocity was obtained by dividing the difference between the two target positions by the radar scan period. This method of initialization reduced the dependance of the filter initialization of target heading and elevation angle information. The filter state vector and initial error covariance matrix are as shown below:

$$\hat{\underline{x}}_0 = \begin{bmatrix} x_t \\ y_t \\ z_t \\ \dot{x}_t \\ \dot{y}_t \\ \dot{z}_t \\ \ddot{x}_t \\ \ddot{y}_t \\ \ddot{z}_t \end{bmatrix} = \begin{bmatrix} x_{tr}(1) \\ y_{tr}(1) \\ z_{tr}(1) \\ (x_{tr}(1) - x_{tr}(0))/T_s \\ (y_{tr}(1) - y_{tr}(0))/T_s \\ (z_{tr}(1) - z_{tr}(0))/T_s \\ 0. \\ 0. \\ 0. \end{bmatrix}$$

(0) initial radar measurement
(1) subsequent radar measurement

$$P_{1i} = \begin{bmatrix} \sigma^2_i & \sigma^2_i/T_s & 0 \\ \sigma^2_i/T_s & 2\sigma^2_i/T_s^2 & 0 \\ 0 & 0 & \beta^2_i \end{bmatrix} \quad ,i = x,y,z.$$

The third initialization scheme for the Kalman filter required three radar downlinks. The interceptor used all three measurements to form the target acceleration. The target velocity was formed using the second and third radar measurements and the target initial position was obtained from the third measurement. The resulting state vector and error covariance matrix is shown below.

$$\hat{\underline{x}} = \begin{bmatrix} x_{tr}(2) \\ y_{tr}(2) \\ z_{tr}(2) \\ (x_{tr}(2) - x_{tr}(1))/T_s \\ (y_{tr}(2) - y_{tr}(1))/T_s \\ (z_{tr}(2) - z_{tr}(1))/T_s \\ (x_{tr}(2) - 2x_{tr}(1) + x_{tr}(0))/T_s^2 \\ (y_{tr}(2) - 2y_{tr}(1) + y_{tr}(0))/T_s^2 \\ (z_{tr}(2) - 2z_{tr}(1) + z_{tr}(0))/T_s^2 \end{bmatrix}.$$

$$P_{2i} = \begin{bmatrix} \sigma^2_i & \sigma^2_i/T_s & \sigma^2_i/T_s^2 \\ \sigma^2_i/T_s & \sigma^2_i/T_s^2 & 3\sigma^2_i/T_s^3 \\ \sigma^2_i/T_s^2 & 3\sigma^2_i/T_s^3 & 6\sigma^2_i/T_s^4 \end{bmatrix} \quad i=x,y,z.$$

The third method demonstrates confidence in the initial "guess" of the target states as noted by the small values created in the error covariance matrix. This confidence level is demonstrated by examining the relative values of the error covariance matrices for the three types of initialization schemes.

Method 1 (position only)

$$P = \begin{bmatrix} 325.2 & 0.0 & 0.0 \\ 0.0 & 1377.9 & 0.0 \\ 0.0 & 0.0 & 96.24 \end{bmatrix}$$

Method 2 (position, velocity)

$$P = \begin{bmatrix} 325.2 & 65.0 & 0.0 \\ 65.0 & 130.0 & 0.0 \\ 0.0 & 0.0 & 96.24 \end{bmatrix}$$

Method 3 (position, velocity, acceleration)

$$P = \begin{bmatrix} 325.2 & 65.0 & 13.0 \\ 65.0 & 130.0 & 7.8 \\ 13.0 & 7.8 & 3.1 \end{bmatrix}$$

7. INITIALIZATION IMPACT ON KEW PERFORMANCE

The launch platform's final task is to launch the interceptor by igniting its main boosters. The interceptor received target position information in downlinks from the radar platform during flight. To control itself, the interceptor employed a divert propulsion scheme utilizing pulse width modulation logic. Upon reaching adequate range, a terminal homing seeker was used to guide the interceptor to hit the target. The initialization process strongly influenced the interceptor's performance because of the errors previously mentioned. Inertial navigation errors, once the interceptor has left the launch platform, can be corrected only if downlink information contains interceptor position information. Since the scenario used in the six degree-of-freedom simulation did not include interceptor position information being passed from the radar platform, the interceptor cannot correct for initial misalignments on-board, and the interceptor is guided off of "true" course. The small IMU misalignments led to large excursions of the interceptor from true position due to the large downrange distances involved inspace-based intercepts. This effect can be seen in the example run in Figure 7 below. The interceptor's divergence from the true course is acceptable if the interceptor can reach a "handover basket" as defined by the terminal homing seeker's field of view. Any initializaiton errors due to

IMU misalignment have been shown to be negated at the terminal phase of flight as no INU information is needed from that point of the flight to intercept.

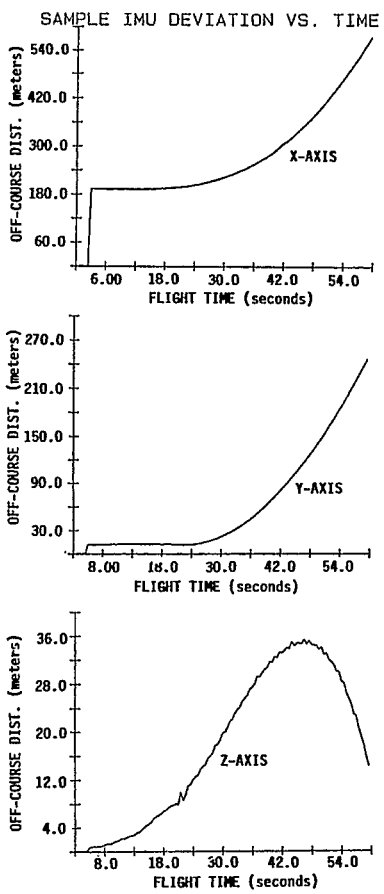

Figure 7: Sample Interceptor Excursions Due to IMU Misalignment

The pointing errors of the interceptor/ launcher described tend to be very visible signs of misalignment as the interceptor's large thrusting vector is skewed from the true thrusting vector, as determined by the pointing algorithm, when that algorithm is corrupted. The misguided interceptor can realize its error during flight when radar downlinks arrive and are decoded, however, the interceptor's large velocity vector along its body X axis is not easily changed by the orthogonal divert forces available for guidance and control. The result of the pointing errors is a condensed kinematic envelope for acquiring targets due to the large amount of propellant used to correct the interceptor's trajectory. Also, results have shown that significant errors in the pointing algorithm can result in "missing" the handover basket altogether as the divert velocity required to attain the handover area is greater than that velocity obtainable from the simulation setup.

The Kalman filter and predictor initialization is the least noticed error added to the initialization process. Because radar platform downlinks occur at the discrete scan points, intermediate corrections are made regarding the target position, velocity, and acceleration vectors. The predictor errors, although small, are fed into the proportional navigation guidance algorithms creating small biases in the guidance commands and eventually to the interceptor's course trajectory. The predictor errors become nulled at the point of handover of guidance from the IMU to the terminal homing seeker. Target information is taken directly (and at a high rate of speed) from the seeker and no predictor is therefore necessary.

8. CONCLUSION

The initialization process as used in the six degree-of-freedom simulation consisted of four subsections. The first subsection included the errors associated with the simulation initialization or the information passed to the launch platform from the radar platform concerning the target information. This initializaiton subsection also included the errors inherent in the launch platform's depiction of its own position, velocity, and acceleration vectors. The second being the initialization of the interceptor inertial navigation unit by defining the platform parameters and adding corresponding errors. The determination of the predicted impact point and the training of the launcher constituted the third initialization routine. And, the initialization and start-up of the on-board Kalman

filter and target predictor completed the launch platform initialization model. These models and their associated errors are but one view of the initialization process, however, the impact of their configuration regarding the interceptor's total flight is apparent. The interceptor six degree-of-freedom simulation shows that errors associated with certian initialization processes can be carried through the flight creating a result that can be detrimental to the interceptor's purpose. For that reason, more modeling and simulation is required in conjunction with alternative SDI architecture studies to determine exactly the extend of initialization errors on total kinetic energy weapon performance.

REFERENCES

Adam, John A. and Wallich, Paul, ed. (September 1985). "SDI: The Grand Experiment", Institute of Electrical and Electronics Engineers Spectrum, 36-64.

Bate, Roger R., Mueller, Donald D. and White, Jerry E. (1971). Fundamentals Of Astrodynamics. Dover Publications, Inc., New York.

Gelb, A. ed. (1974). Applied Optimal Estimation. The MIT Press, Cambridge, Mass.

The Analytic Sciences Corporation (TASC). (March 1981). Report TR-3218-1. "Strapdown Inertial Midcourse Guidance for Air Defense Missiles"

AUTHORS' BIOGRAPHIES

WILLIAM A. LAIDIG is a system analyst with Science Applications International Corporation. He received a B.S. in Electrical Engineering from Auburn University in 1982 and a M.S. in Control Theory from Auburn University in 1985. Current research projects include control, analysis, and simulation of space-based and ground launched endoatmospheric non-nuclear defense weapons.

DR. HAROLD L. PASTRICK holds degrees from Carnegie-Mellon, Stanford, and California Western Universities. He is Assistant Vice President of Science Applications, Incorporated, responsible for technical support to major tactical weapon systems under development by the U.S. Army and Air Force. He previously was Vice President for Engineering and Consulting Engineer for the Control Dynamics Company involved in weapon systems research and engineering. His background in tactical systems began in 1958 at the Laboratories of the U.S. Army Electronics Command, where he was active in developing avionics systems for Army helicopters. He later joined the U.S. Army Missile Command, where he was involved in research, development, and evaluation of guidance and control systems for most of the Army's terminally guided tactical missiles. In 1976, he became staff Specialist and Assistant to the Director, Land Warfare, Office of the Under-Secretary of Defense for Research and Engineering, with responsibilities for managing, researching, developing, and acquiring major weapon systems in the tactical warfare area. He has published over 90 technical papers in the analysis of weapon systems-guidance, navigation, and control and on missile simulation techniques. He is a registered Professional Engineer in the state of Alabama, a Lecturer in the School of Science and Engineering at the University of Alabama in Huntsville, Lecturer and Research advisor at the Southeastern Institute of Technology, Huntsville, Alabama, and Lecturer at the George Washington University, Washington, D.C. He has given lectures and seminars on tactical guided weapons and simulation modeling in the industrial setting, academia, and professional colloquia in Canada, Mexico, Europe and throughout the U.S.A.

William A. Laidig
Dr. Harold L. Pastrick
Science Applications International Corporation
2109 West Clinton Avenue, Suite 800
Huntsville, Alabama 35801
(205) 533-5900